

# ARE POLYNOMIAL MODELS OPTIMAL FOR IMAGE INTERPOLATION?

*Hagai Kirshner and Moshe Porat*

Department of Electrical Engineering, Technion–Israel Institute of Technology, Haifa 32000, Israel

phone: + (972) 4-8293283, fax: + (972) 4-8294709

email: kirshner@tx.technion.ac.il, web: <http://visl.technion.ac.il/kirshner>

phone: + (972) 4-8294684, fax: + (972) 4-8295757

email: mp@ee.technion.ac.il, web: <http://visl.technion.ac.il/mp>

## ABSTRACT

A reproducing-kernel Hilbert space approach to image interpolation is introduced. In particular, the reproducing kernels of Sobolev spaces are shown to be exponential functions that give rise to alternative interpolation kernels. Both theoretical and experimental results are presented, indicating that the proposed exponential functions perform better in terms of SNR and of boundary-effects removal than currently available methods, in particular polynomial-based kernels, while introducing no additional computational overhead.

## 1. INTRODUCTION

Interpolation is needed in several image processing tasks such as rotation, translation, resizing and derivative evaluation. The underlying idea in current linear interpolation methods corresponds to regularity constraints that are imposed on the continuous-domain image where the pixel values provide its sampled version. For example, sinc-based interpolation kernels assume bandlimitedness (apodized sinc, discrete sinc) while other methods assume piecewise polynomial models (nearest neighbor, linear, Schaum, Keys, Dodgson, B-spline, Meijering and OMOMS [1, 2]). Every model converges to the original function as the sampling interval shortens and the corresponding approximation error can be characterized by [1]:

$$\|\mathbf{x} - \hat{\mathbf{x}}\|_{L_2} \propto C \cdot \Delta^L \cdot \|\mathbf{x}^{(L)}\|_{L_2}. \quad (1)$$

Here,  $\mathbf{x}$  is the original continuous domain signal,  $\mathbf{x}^{(L)}$  is its  $L$ th derivative,  $\hat{\mathbf{x}}$  is the interpolated signal and  $\Delta$  is the sampling interval. In such a formulation, the parameters  $L$  and  $C$  are the approximation order and the proportional constant, respectively; and they provide a means for comparing the various reconstruction (interpolation) methods. Both theoretical and experimental studies have shown that the piecewise-polynomial B-spline kernels perform better than other currently available designs [3].

Non-linear interpolation methods correspond to edge-directed methods [4–7], to wavelet transform operations [8, 9] and to PDE (Partial Differential Equation) models [10] to name a few. These methods impose additional constraints on the continuous-domain signal. Edge-directed methods spatially adapt the interpolation coefficients to better match local structures around edges. Multiresolution approaches aim at properly modeling the wavelet coefficients of higher resolutions based on the given low resolution image. Possible models are an exponential decay at different scales or the mixture of Gaussians model imposed on the wavelet coefficients. Super resolution approaches also use additional information within the wavelet domain. This information, however, often relies on training data sets rather than on an analytic model. These adaptive methods aim at improving the subjective quality of the interpolated image rather than minimizing the error measure of (1). They rely on training

data sets and on iterative algorithms, as well as on statistical models. This, in turn, gives rise to increased computational complexity and to possibly poor performance for images that do not properly fit the imposed model. Also, these methods are often restricted to dyadic resolution enhancement and may be found less suitable for practical applications.

Focusing on the error measure of (1), an alternative linear interpolation approach is introduced in which a less restrictive constraint is imposed on the continuous-domain signal. It is suggested here to use the Sobolev space framework for this purpose. Sobolev spaces consist of smooth functions and they serve as the underlying continuous-domain model in several image processing tasks [11–13]. Further, Sobolev functions are dense in  $L_2$  and they can properly approximate an arbitrary continuous-domain finite-energy signal. It seems, however, that the reproducing-kernel Hilbert space (RKHS) property of these spaces has not been investigated within the context of image interpolation. It will be shown that this property produces exponential-based interpolation kernels having attractive properties in terms of approximation error characterization while experimental results will further support these findings.

## 2. EXPONENTIAL-BASED INTERPOLATION FUNCTIONS

Let  $H_2^p$  be the Sobolev space of order  $p$ . This space consists of all one-dimensional finite-energy functions defined on the real line for which their first  $p$  derivatives are of finite energy as well. The corresponding inner product is given by

$$\langle \mathbf{x}, \mathbf{y} \rangle_{H_2^p} = \sum_{n=0}^p \lambda_n \cdot \langle \mathbf{x}^{(n)}, \mathbf{y}^{(n)} \rangle_{L_2}, \quad (2)$$

where  $\{\lambda_n\}$  is an arbitrary set of positive numbers and

$$\langle \mathbf{x}, \mathbf{y} \rangle_{L_2} = \int_{-\infty}^{\infty} \mathbf{x}(s) \cdot \mathbf{y}(s) ds. \quad (3)$$

It then follows that the reproducing kernel of  $H_2^p$  is given by

$$\varphi(s, t) = \mathcal{F}^{-1} \left\{ \frac{1}{\lambda_0 + \lambda_1 \omega^2 + \dots + \lambda_p \omega^{2p}} \right\} (s - t), \quad (4)$$

where  $\mathcal{F}^{-1}$  denotes the inverse Fourier transform operation. Recalling the binomial coefficients, one may choose  $\lambda_n = \binom{p}{n}$  to yield

$$\varphi(s, t) = \mathcal{F}^{-1} \left\{ \frac{1}{(1 + \omega^2)^p} \right\} (s - t). \quad (5)$$

The ensued kernels correspond to exponential functions and they are given in Table 1. Other choices for  $\{\lambda_n\}_n$  will not be

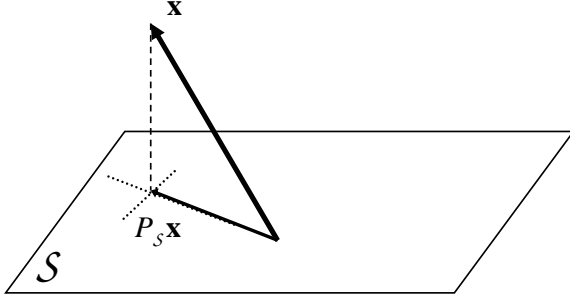


Figure 1: A vector interpretation of the ideal sampling process in a Sobolev space.  $\mathcal{S}$  is the sampling space. It is determined by the exponential reproducing kernel of the Sobolev space and by the sampling points.  $P_{\mathcal{S}}\mathbf{x}$  is the known portion of the continuous-domain signal  $\mathbf{x}$  that is captured by the sampling process.

Table 1: Reproducing kernels of Sobolev spaces.

Sobolev order	$\varphi(s, t)$
1	$\frac{1}{2} e^{- s-t }$
2	$\frac{1}{4} e^{- s-t } \cdot [1 +  s-t ]$
3	$\frac{1}{16} e^{- s-t } \cdot [3 + 3 s-t  +  s-t ^2]$

considered here. Being an RKHS, the Sobolev space framework suggests an orthogonal projection interpretation for the ideal sampling process [14, 15]. Let  $\mathbf{x}(t)$  be an arbitrary Sobolev function and let  $\Lambda = \{t_n\}_n$  be a set of sampling points. It then follows that the sample values satisfy

$$\mathbf{x}(t_n) = \langle \mathbf{x}(\cdot), \varphi(\cdot, t_n) \rangle_{H_2^p}, \quad (6)$$

while the set of functions  $\{\varphi(\cdot, t_n)\}_n$  constitutes a Riesz basis for their span

$$\mathcal{S} = \overline{\text{Span}}\{\varphi(\cdot, t_n)\}. \quad (7)$$

The corresponding Gram matrix is given by

$$G(m, n) = \varphi(t_m, t_n), \quad (8)$$

and the orthogonal projection of  $\mathbf{x}$  onto the sampling space is given by

$$P_{\mathcal{S}}\mathbf{x} = \sum_n a_n \cdot \varphi(\cdot, t_n). \quad (9)$$

Here,  $a = G^{-1}c$  while  $c$  denotes the ideal samples of  $\mathbf{x}$  on  $\Lambda$ . The unknown portion of  $\mathbf{x}$  that is not captured by the sampling process is  $P_{\mathcal{S}^\perp}\mathbf{x} = \mathbf{x} - P_{\mathcal{S}}\mathbf{x}$  (Figure 1). In shift-invariant cases, where  $\Lambda$  consists of an infinite number of uniformly-spaced sampling points,  $G^{-1}$  can be replaced by a proper digital filter; this filter has a rational transfer function originating from the exponential terms that compose  $\varphi(s, t)$ .

The sample sequence  $c$  may be interpreted by means of the representation coefficients of  $P_{\mathcal{S}}\mathbf{x}$  with respect to the bi-orthogonal set of  $\{\varphi(\cdot, t_n)\}_n$ . That is,

$$P_{\mathcal{S}}\mathbf{x} = \sum_n c_n \cdot \psi_n(s), \quad (10)$$

where bi-orthogonality is taken in the Sobolev sense. i.e.,

$$\psi_n(s) = \sum_m G_{n,m}^{-1} \cdot \varphi(s, t_m). \quad (11)$$

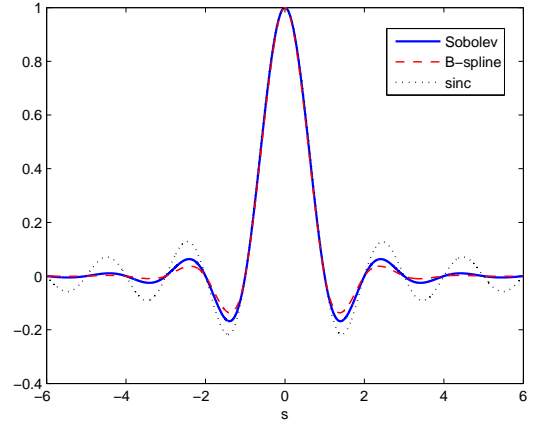


Figure 2: Sobolev (solid), cubic B-spline (dashed) and sinc (dotted) interpolation functions for a unit sampling step. The Sobolev order is  $p = 3$ .

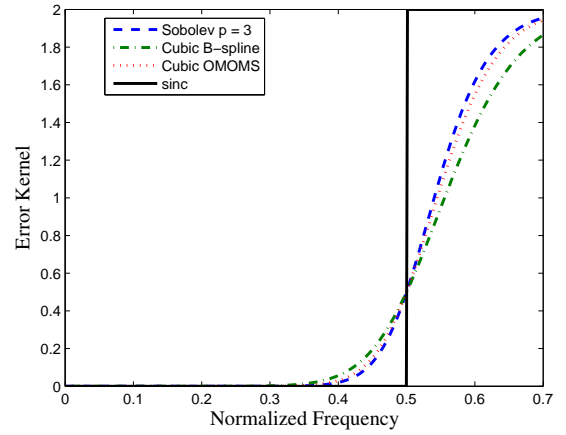


Figure 3: Error kernel for Sobolev (dashed), for B-spline (dash-dotted), for OMOMS (dotted) and for the sinc (solid) functions. The parameter  $p = 3$  denotes the Sobolev order.

Each function  $\psi_n$  is composed of a weighted sum of shifted exponential functions and owing to the RKHS property of  $H_2^p$  they are interpolative. Figure 2 compares these exponential-based interpolating functions with their B-spline counterparts and with the sinc function. Unlike currently available interpolation kernels, the proposed functions do not comply with the partition-of-unity condition although this condition is asymptotically met as the Sobolev order  $p$  increases.

When modifying the sampling grid, the ensued interpolating functions  $\{\psi_n\}_n$  scale accordingly. This scaling property does not apply, however, to the exponential functions  $\{\varphi_n\}_n$ , which remain unscaled but align themselves to the new grid instead. Nevertheless, both  $\{\varphi_n\}_n$  and  $\{\psi_n\}_n$  span the same sampling space  $\mathcal{S}$ . In this regard, the error kernel introduced in [1] for the shift-invariant case provides a means for comparing between various generating functions (interpolative and non-interpolative). It describes the average  $L_2$  error between the original function and its interpolated version where averaging is taken over all possible phase shifts

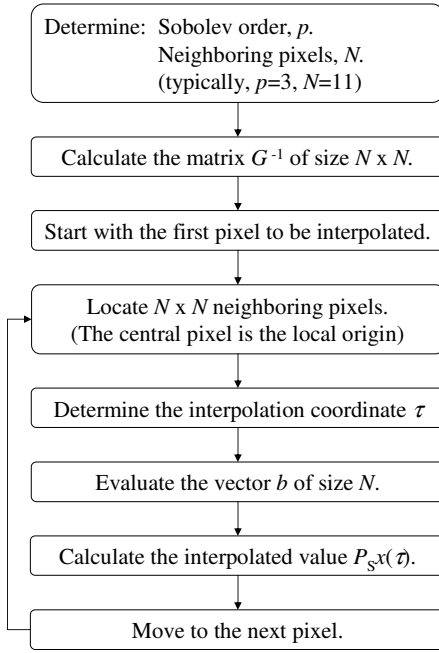


Figure 4: A flow chart of the proposed interpolation method.

of the sampling grid. This kernel is given by

$$E(\omega) = \frac{\left| \sum_{k \neq 0} \Phi(\omega + 2\pi k) \right|^2 + \sum_{k \neq 0} |\Phi(\omega + 2\pi k)|^2}{\left| \sum_{k=-\infty}^{\infty} \Phi(\omega + 2\pi k) \right|^2}, \quad (12)$$

where  $\Phi$  denotes the Fourier transform of  $\varphi$ . Figure 3 depicts this kernel for several generating functions, showing that the proposed exponential functions introduce less approximation error than the B-spline and the OMOMS functions at the required lower frequency band. Unlike other piecewise polynomial functions, however,  $E(\omega)$  of the proposed exponential functions does not equal zero at the origin although it converges to this value as the Sobolev order  $p$  increases.

The reproducing kernel of a two-dimensional Sobolev space is not a separable function. The Fourier transform of such kernels is given by  $\Phi(u, v) = 1/(1+u^2+v^2)^p$ ,  $p \geq 2$  and the radially symmetric space-domain kernels are given by  $\varphi(r) = 2\pi^p r^{p-1} K_{p-1}(2\pi r)/\Gamma(p)$  where  $r^2 = x^2 + y^2$ ,  $K_n(\cdot)$  denotes the Bessel function of the third kind of order  $n$  and  $\Gamma$  is the gamma function. Nevertheless, a separable model allows for a relatively short run-time implementation that is comparable with other linear interpolation methods and is therefore adopted in this work as well.

### 3. COMPUTATIONAL COMPLEXITY

The Gram matrix formulation of (9) is preferable over the oftenly used shift-invariant structure due to the finite rather than an infinite number of samples that are available for an image. In such a formulation, the evaluation of the matrix  $G^{-1}$  in (9) introduces a negligible computational overhead for images of standard size. Notwithstanding, the significant values of  $G^{-1}$  are located near the main diagonal and large images may be interpolated by considering a relatively small neighborhood of pixels. Therefore, the proposed interpolation approach requires an off-line evaluation of  $G^{-1}$  having a relatively small size and it evaluates a single pixel by the following finite-dimensional discrete-domain inner product

$$P_S \mathbf{x}(\tau) = \mathbf{c} \cdot G^{-1} \cdot \mathbf{b}. \quad (13)$$

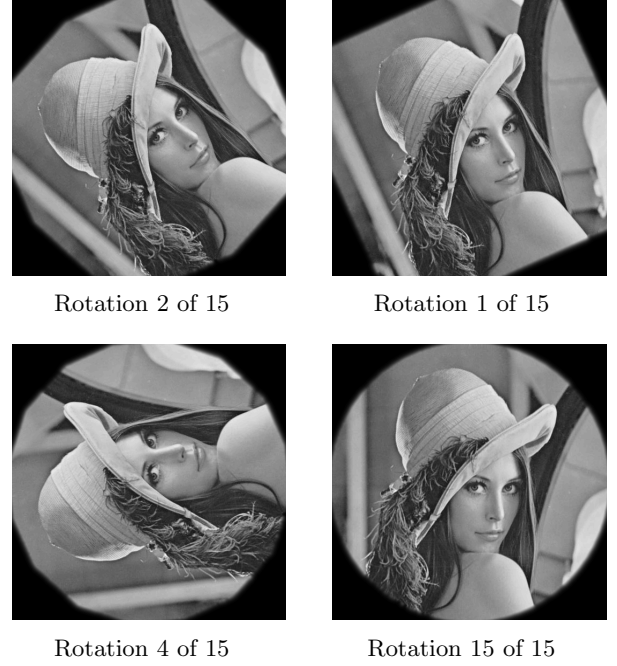


Figure 5: An example of an image rotation using the proposed exponential-based interpolation functions. Further image details are shown in Figure 7.

Here,  $\tau$  is the interpolation coordinate,  $P_S \mathbf{x}(\tau)$  is interpolated value,  $\mathbf{c}$  is an  $N$ -dimensional vector corresponding to the values of neighboring pixels located at  $\{t_n\}$ , and  $b_n = \varphi(\tau, t_n)$  corresponds to  $N$  samples of the reproducing kernel of  $H_2^p$ . The size of  $G^{-1}$  is  $N \times N$  and it is given in (8). In practice, the choice of  $N = 11$  was shown to be adequate for a Sobolev model of  $p = 3$ . Every interpolated pixel is separately evaluated by identifying its neighbors  $\mathbf{c}$ , by identifying its relative location within this neighborhood  $\tau$ , and by applying (13) to yield its value. Figure 4 further depicts a flow chart of the algorithm. As for two-dimensional signal interpolation, the separability assumption enables one to apply

$$P_S \mathbf{x}(\tau_x, \tau_y) = \mathbf{b}_y^T \cdot G^{-1} \cdot \mathbf{c} \cdot G^{-1} \cdot \mathbf{b}_x. \quad (14)$$



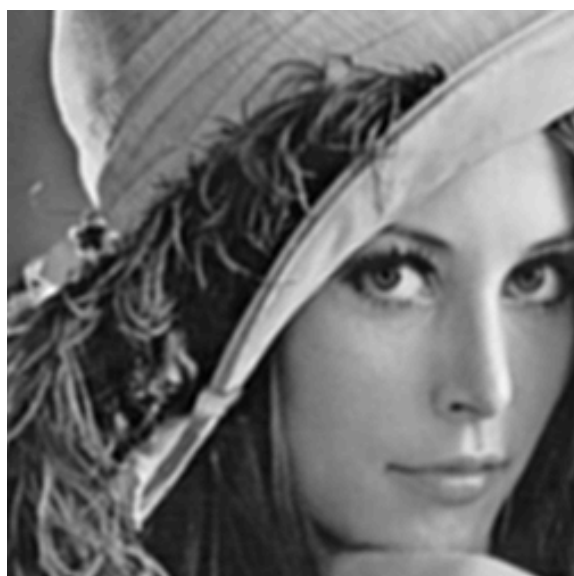
Figure 6: Cardiac MRI image. Further image details are shown in Figure 7.



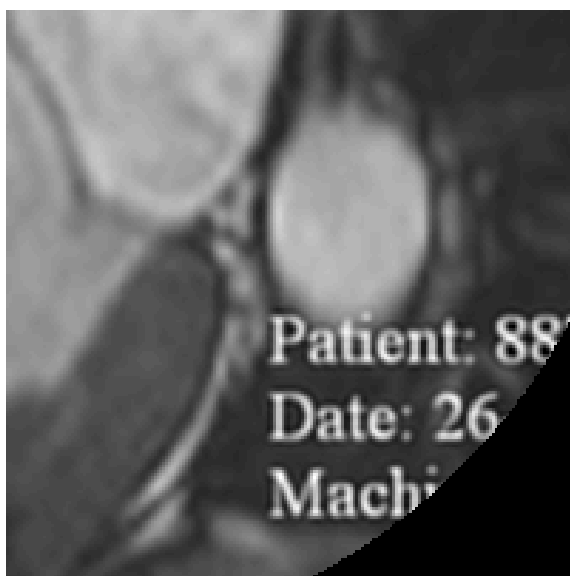
Lena



Cardiac MRI



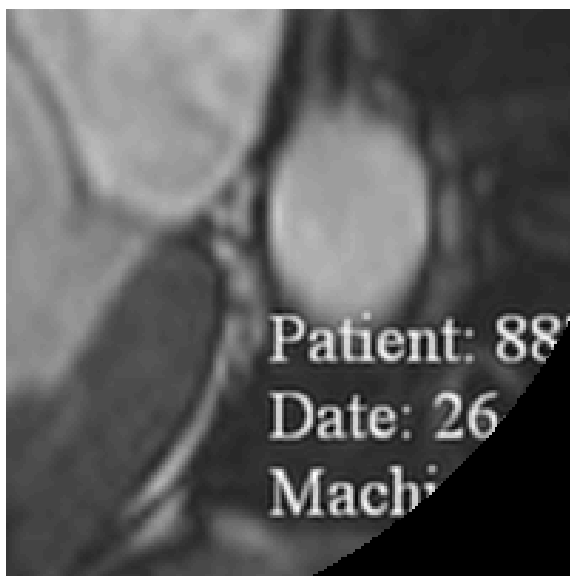
B-spline, SNR = 28.6[dB]



B-spline, SNR = 22.1[dB]



Sobolev, SNR = 31.7[dB]



Sobolev, SNR = 24.3[dB]

Figure 7: An image rotation experiment. Shown are portions of Lena (first column) and of the Cardiac MRI image (second column). SNR values correspond to full image data having applied 100 rotations of  $3.6^\circ$  each. The cubic B-spline model is compared with the proposed exponential-based interpolation kernel while assuming a Sobolev order of  $p = 3$ .

The proposed approach is similar to linear interpolation methods. These methods are also composed of a pre-filtering stage for extracting proper representation coefficients and of a pointwise evaluation of the continuous-domain signal at the required grid. It then follows that the computational complexity of the proposed approach is similar to convolution-based interpolation methods while no iterative algorithm or a-priori knowledge is required for the task at hand. It is noted here that when considering piecewise-polynomial models, the proposed exponential-based model requires several additional floating-point operations per pixel due to the exponential kernels  $\varphi$  that are being evaluated during the interpolation process.

#### 4. EXPERIMENTAL RESULTS

The proposed exponential kernel have been compared with the cubic B-spline interpolation function while considering a Sobolev order of  $p = 3$ . Cubic B-spline interpolation provides a good cost-performance trade off and was therefore chosen. The proposed method and the B-spline method were both implemented using a Gram matrix formulation. Such an implementation was shown to yield SNR values of almost 2[db] better for the B-spline model than digitally filtering the image as suggested in [1]. This Gram matrix formulation does not require extracting the image by its mirror version either.

Following [1], successive image rotations were applied to an image until it reached its starting position allowing for an SNR value calculation. Figure 5 depicts several such rotations using the proposed interpolation function. The proposed method was shown to yield better SNR values than the values obtained by the B-spline method. Considering the image of Lena, for example, 15 rotations of  $24^\circ$  each, yield an SNR value of 36.5[db] compared to 33.9[db]. Such an experiment was also conducted in [1] where an SNR value of 32.0[db] was reported for digitally filtering the image by a cubic B-spline model, and where a value of 34.29[db] was reported for the piecewise polynomial cubic OMOMS (optimal maximal order minimal support) model. Also, the cardiac MRI image (Figure 6) was shown to yield SNR values of 28.1[db] compared to 26.0[db]. Similar results were obtained for other images [16] suggesting that the proposed exponential-based model may perform better than piecewise-polynomial functions. In this regard, it is noted that the proposed method outperformed the cubic B-spline and the cubic OMOMS methods for all images that have been examined in this work. Figure 7 further suggests that the proposed functions may visually preform better as well. SNR values were calculated based on a circular region having a diameter of 90% of the image's dimensions. Nevertheless, when considering larger circular areas, boundary effects lead to more prominent results in favor of the proposed exponential functions [16].

#### 5. CONCLUSIONS

A reproducing-kernel Hilbert space approach has been proposed for image interpolation. Sobolev (smooth) functions are dense in  $L_2$  providing a very useful framework for this purpose. The reproducing kernels of these Sobolev spaces are shown to be exponential rather than polynomial functions and the ideal sampling process is characterized by a set of proper inner products. These kernels also give rise to interpolation functions that outperform currently available methods while introducing no additional computational overhead. Theoretical and experimental results have been presented involving image rotation. Our conclusion is that the proposed method could provide a better alternative to the use of B-spline kernels and to the use of piecewise-polynomial models for convolution-based image interpolation while introducing no additional computational overhead.

#### ACKNOWLEDGMENTS

This work was supported in part by a grant from the GIF, the German-Israeli Foundation for Scientific Research and Development, by the Eshkol Fund of the Israeli Ministry of Science, and by the Ollendorff Minerva Centre. Minerva is funded through the BMBF.

#### REFERENCES

- [1] T. Blu, P. Thévenaz, and M. Unser, "MOMS: Maximal-order interpolation of minimal support," *IEEE Trans. Image Processing*, vol. 10, pp. 1069–1080, July 2001.
- [2] J. Shi and S. E. Reichenbach, "Image interpolation by two-dimensional parametric cubic convolution," *IEEE Trans. Image Processing*, vol. 15, no. 7, pp. 1857–1870, July 2006.
- [3] E. H. W. Meijering, W. J. Niessen, and M. A. Viergever, "Quantitative evaluation of convolution-based methods for medical image interpolation," *Med. Image Anal.*, vol. 5, no. 2, pp. 111–126, 2001.
- [4] J. P. Allebach, *Image Scanning, Sampling and Interpolation*. San Diego, Ca.: Academic, 2000, ch. 7.1, pp. 629–643.
- [5] X. Li and M. Orchard, "New edge-directed interpolation," *IEEE Trans. on Image Processing*, vol. 10, no. 6, pp. 1521–1527, June 2001.
- [6] A. Gotchev, K. Egiazarian, J. Vesma, and T. Saramäki, "Edge-preserving image resizing using modified b-splines," in *IEEE International Conference on Acoustics, Speech, and Signal Processing (ICASSP)*, 2001.
- [7] Y. Cha and S. Kim, "Edge-forming methods for color image zooming," *IEEE Trans. Image Processing*, vol. 15, no. 8, pp. 2315–2323, August 2006.
- [8] C. V. Jiji, M. V. Joshi, and S. Chaudhuri, "Single-frame image super-resolution using learned wavelet coefficients," *International Journal of Imaging Systems and Technology*, vol. 14, no. 3, pp. 105–112, 2004.
- [9] X. Li, "Image resolution enhancement via data-driven parametric models in the wavelet space," *EURASIP Journal on Image and Video Processing, Volume 2007, Article ID 41516, 12 pages*, 2007.
- [10] H. Aly and E. Dubois, "Image up-sampling using total-variation regularization with a new observation model," *IEEE Trans. on Image Processing*, vol. 14, no. 10, pp. 1647–1659, October 2005.
- [11] T. F. Chan and J. Shen, *Image Processing And Analysis: Variational, PDE, Wavelet, And Stochastic Methods*. SIAM, 2005.
- [12] B. Burgeth, S. Didas, and J. Weickert, "The bessel scale-space," in *Deep Structure, Singularities, and Computer Vision*, O. F. Olsen, L. Florack, and A. Kuijper, Eds. Berlin: Springer, 2005, pp. 84–95.
- [13] H. Kirshner and M. Porat, "On interpolation of differentially structured images," in *European Signal Processing Conference (EUSIPCO)*, 2007.
- [14] —, "On the approximation of  $L_2$  inner products from sampled data," *IEEE Trans. Signal Processing*, vol. 55, no. 5, pp. 2136–2144, May 2007.
- [15] T. G. Dvorkind, H. Kirshner, Y. C. Eldar, and M. Porat, "Minimax approximation of representation coefficients from generalized samples," *IEEE Trans. Signal Processing*, vol. 55, no. 9, pp. 4430–4443, September 2007.
- [16] H. Kirshner and M. Porat, "On the role of exponential functions in image interpolation," Technion, CCIT Report 683, January 2008.